Improving Interference Cancellation in Spatial Division Multiplexing Using a Combination of the Channel Coding and QR-Successive Interference Cancellation

Heba Talla Adel Ibrahem[1], Ashraf Yehya Hassan[1], and Abdelhalim zekry[2]
[1] Benha Faculty of Engineering, Benha University, Benha, Egypt
[2] Ain Shams University-Faculty of Engineering, Benha University, Egypt
Email: hebatalla780@gmail.com, Ashraf.fahmy@bhit.bu.edu.eg, AaaZekry@hotmail.com

***Abstract*—**This paper introduces QR-SIC detector to minimize the probability of error comparing to SDM system. Spatial-division-multiplexing (SDM) system is a multiple-inputs-multiple-outputs (MIMO) system used to increase data transmission rate in modern communication systems. The major disadvantage of SDM system is the interference between the received symbols. In this paper, a new trans-receiver architecture for SDM system is introduced. This receiver uses a Successive-Interference-Cancellation (SIC) detector based on QR-decomposition of the channel matrix and a Forward-Error-Correction (FEC) channel code. The proposed architecture merges the interference cancellation process in QR-SIC detector and the forward error correction process in the channel decoder. The feedback symbols in the QR-SIC detector are the output symbols from the channel decoder after they are re-encoded and re-modulated and more robust. The new architecture minimizes the probability of error in the demodulated symbols more than the conventional SDM receiver. If the conventional SDM receiver needs 100 MWATT transmitted power the proposed system needs only 64 MWATT transmitted power. So The new architecture of the SDM receiver can save up to 36% of the transmitted signal power used with the conventional SDM receiver. At BER of 10^{-4}, the convolution codes of code rates 3/4, 1/2, and 1/4 achieve coding gains of 15 dB, 24 dB, and 30 dB with respect to the uncoded 4-antennas SDM receiver. the proposed SDM receiver at BER of 10^{-4} is 2dB, 1.5 dB, and 0.9 dB better than the BER performance of the conventional coded SDM receiver at the same code rates and the same number of antenna. The enhancement in the BER performance of the proposed SDM receiver increases as the code gain of the used code. This increase in the power efficiency and bandwidth comes at the expense of an increase in the receiver complexity and latency

Index Terms—Spatial multiplexing, Multiplexing interference, Successive interference cancellation. Channel matrix, QR decomposition, Channel codes

I. INTRODUCTION

The most important technology in broadband wireless communication systems is MIMO technology especially SDM (spatial division multiplexing system. The proposed SDM system offers high data rate and small probability of error by using more robust feedback symbols. Speaking of data rate, increasing the rate of the transmitted data is a major requirement in modern communication systems. Three methods are usually used to increase this rate. These methods are done in time domain, frequency domain, and spatial domain. The first method is the simplest one and it is done in the time domain. It uses a single carrier modulation, and the data rate is increased by reducing the symbol period. This method increases the bandwidth of the modulated signal as well as the rate of the transmitted data. The coherent bandwidth of the channel limits the modulated signal bandwidth and the data transmission rate. Inter-Symbol Interference (ISI) appears between the received symbols when the modulated signal bandwidth exceeds the coherent bandwidth of the channel. The channel equalization is usually used in the receiver to remove or minimize the ISI signal. Although the channel equalization compensates the effects of the bandwidth limitation of the channel, it increases the complexity of the receiver. The new work in [1] shows that the ISI signal can be exploited to enhance the Bit-Error-Rate (BER) performance of the receiver in the fading channel without any limitations on the transmitted data rate. However, the complexity of the proposed receiver in this work is higher than the complexity of the conventional receivers used to minimize the ISI signal. The second method of increasing the data rate is done in the frequency domain. This method uses multi- carrier modulation. N parallel subcarriers are used to transmit N independent symbols, simultaneously. The maximum achievable transmission rate in this system is equal to the maximum achieved rate on one subcarrier multiplied with the number of used parallel subcarriers. To solve the ISI problem in the multi-carrier system, the bandwidth of the modulated signal in each sub-channel is adjusted to be smaller than the coherent bandwidth of the transmitting channel [2]. The multi-carrier system suffers from inter-carrier interference (ICI) when the N used subcarriers are not orthogonal. Orthogonal-Frequency-Division-Multiplexing (OFDM) system is proposed to solve the ICI problem in multi-carrier systems. The subcarriers in the OFDM system are orthogonal and no ICI

Manuscript received December 15, 2021; revised June 15, 2022.
doi:10.12720/jcm.17.7.528-540

appears between the sub-channels. When the channel suffers from Doppler frequency shift, or there is a miss-synchronization between the received signal and the local carriers in the receiver, the orthogonality between the subcarriers in the OFDM signal is lost. In this case, ICI appears again, and it should be removed or minimized by the receiver [3], [4]. OFDM is used in many applications, where high data rate is required such as the fourth and fifth generations of cellular networks and the Digital Video Broadcasting (DVB) standards. The third method of increasing the rate of the transmitted data is done in the spatial domain. This method uses SDM system. This system transmits N independent modulated symbols over N transmitting antennas, simultaneously. The single carrier modulation as well as the multi-carrier modulation can be used with the SDM system. To achieve the required capacity gain, the number of the receiving antennas and the number of the independent paths from the transmitter to the receiver must be greater than or equal to the number of the transmitting antennas [5], [6]. The SDM system is not like the spatial diversity MIMO system. The first uses the multiple transmitting and receiving antennas to increase the system capacity. However, the later uses the multiple transmitting and receiving antennas to increase the reliability (diversity gain) of the system [7]. The SDM system suffers from the interference between the received symbols. The space-time codes may be used in the transmitter to get orthogonal symbols on the transmitting antennas. This removes the interference between the received symbols, however the redundancy in the space-time codes reduces the capacity of the MIMO system [8]. The other method of removing or reducing the interference in the SDM system is the using of the interference cancellations detectors. The maximum- likelihood (ML) interference cancellation detector is the optimum interference cancellation detector, which removes the interferences between the received symbols in SDM receivers. However, the complexity of the ML detector grows exponentially with the number of the interfering symbols [9]. Linear interference cancellation detectors are often used in SDM receivers, because their complexities increase linearly with the number of the interfering symbols. However, the linear interference cancellation detectors are sub-optimum detectors. Linear interference cancellation is usually done in a parallel way or in a successive way. The Parallel Interference Cancellation (PIC) detectors such as the zero-forcing detector (ZF) and the Minimum-Mean-Square-Error (MMSE) detector remove the interference between the N multiplexed symbols in the received vector concurrently [10]-[12]. The ZF detector removes the interference completely, but it increases the power of the received noise. The MMSE detector compromises between the interference cancelation and the enhancement of the received noise power. The achievable sum rate for MMSE is improved based on the distributed users inside cell, mitigated the inter-cell interference caused when send the same signal by other cells. By contrast, MMSE is better than ZF in perfect Channel State Information (CSI) for approximately 20% of the achievable sum rate [13]. The second group of the linear interference cancellation detectors is the successive interference cancellation (SIC) detectors. In these detectors, a decision is made about an interfering symbol, and then this symbol is subtracted from the other interfering symbols. This process is repeated until all the interfering symbols are detected [14], [15]. This procedure removes the interference if the decision of the detected symbol is correct; otherwise, it will duplicate the contribution of the interference. Although linear detectors suffer from mediocre performance, the ZF method and the MMSE method are found to play a crucial role in the receiver design due to their relative simplicity [16]. The last group of the interference cancellation detectors is the decision feedback (DF) detectors [17], [18]. These detectors are nonlinear detectors. In the DF detectors, a linear matrix maps the received symbols to the decision vector. This mapping may be based on the ZF criterion or the MMSE criterion. It removes a large amount of the interference from the received symbols. A decision device is used to detect the symbols from the decision vector. These symbols are returned back to the input of the decision device after remapping with another mapping matrix. The remapped vector is subtracted from the input of the decision device to remove the residual interference. The performance of the DF detectors is better than the performance of the linear detectors [19], [20]. However, the complexity of the DF detectors is higher than the complexity of the linear detectors. Recently, Cooperative MIMO (CO-MIMO) employs multiple surrounding BS to jointly transmit and receive signals to and from users. This prevents inter-cell interference in neighboring BS as may be experienced with traditional MIMO systems [21].

In this paper, a new architecture is proposed for SDM receiver. The proposed receiver uses QR-SIC detector to remove the interference between the received symbols. The FEC channel coding is also used to enhance the BER performance of the proposed SDM receiver. In the new architecture, the function of the QR-SIC detector is merged with the function of the channel decoder. The feedback symbols to the QR-SIC detector are the corresponding symbols to output symbols from the channel decoder after they are re-encoded and re-modulated. However, in the conventional SDM receiver, the feedback symbols to the QR-SIC detector are the outputs symbols from the previous stages in the QR-SIC detector. The probability of error in the received symbols after the channel decoder is smaller than the probability of error in the received symbols after the QR-SIC detector. Therefore, the feedback in the QR-SIC detector of the proposed receiver is done by more robust symbols, however the feedback in the QR-SIC detector of the conventional SDM receivers is done by less robust symbols. In this work, the BER performance of the proposed SDM receiver is compared with the BER performance of the conventional SDM receiver with the

same channel coding and QR-SIC detector. The signal to interference power ratio (SIR) in SDM system is usually less than one (0 dB). FEC channel codes with high code gains are used to enhance the BER performance in the conventional and the proposed SDM receivers. The convolution code, the turbo code, and the low-density parity check code (LDPC) are examples of these codes, which work well in the channels with low SIRs. Since the BER performance of the LDPC code is very close to the Shannon limit [22], this gives the motivation to introduce a new mathematical method to generate the parity check matrix of the LDPC codes. The proposed method generates the parity check matrix for the LDPC codes, which are used in the simulated systems. A full study of the proposed method for generating the parity-check matrix of the LDPC code will be done in a separate paper to prevent the prolongation of the current one. Section II shows the mathematical model of the SDM signal and the conventional SDM transmitter. The architecture of the SDM transmitter and the proposed architecture of the SDM receiver are represented in this section. A trace of the received symbols in all the parts of the proposed receiver is also introduced. In Section III, the suggested algorithm for generating the parity check matrix of the used LDPC code that will be used with the proposed receiver, is introduced. The specifications of the used channel models and the simulations of the conventional and the proposed SDM receiver are shown in Section IV. The simulation results, the discussions and conclusion are presented in this section too.

II. The Proposed QR-SIC Detector for SDM System

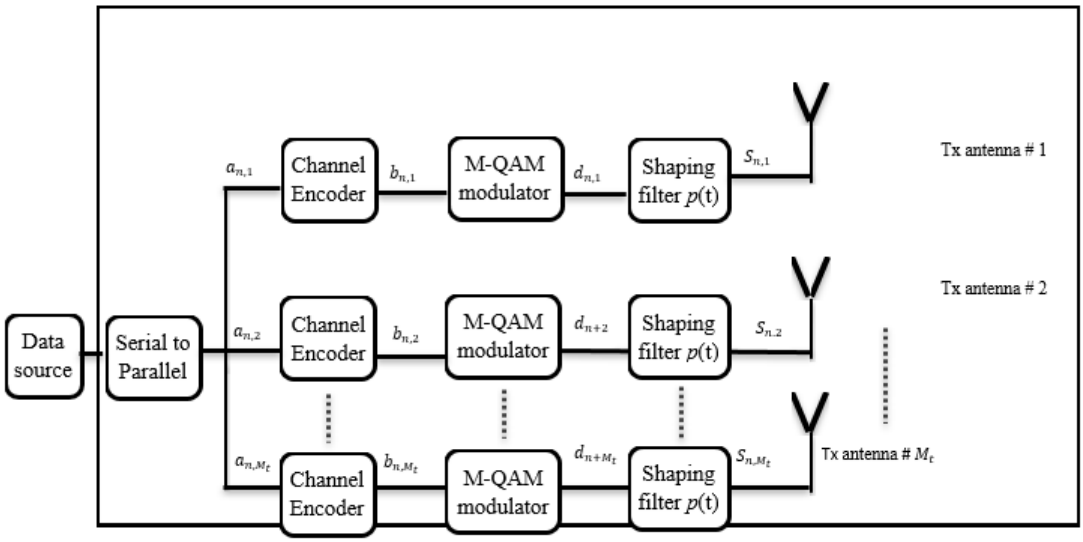

Fig. 1. A block diagram of an SDM transmitter with LDPC encode

In the conventional SDM receiver, the feedback symbols to the interference cancellation detector come from the outputs of the previous stages in the detector. The channel decoder is independently used to correct the errors in the demodulated symbols after the interference cancellation detector. In the proposed SDM receiver, integration between the channel decoder and the interference cancellation detector is made, where the feedback is done from the output of the channel decoder to the input of the interference cancellation detector. The proposed SDM receiver uses QR-SIC detector to remove the interferences between the received symbols. The QR-SIC detector uses the QR-decomposition algorithm to decompose the channel matrix of the SDM system. It removes the interference between the received symbols in sequence one by one. The first detected symbol from the first stage of the QR-SIC detector is not directly fed to the input of the next stage. It is demodulated and then applied to the channel decoder. The channel decoder corrects some of the errors in the demodulated symbol. At this stage, the probability of error in the first detected symbol after the channel decoder is smaller than the probability of the error in the corresponding symbol at the output of the QR-SIC detector. The first symbol after the channel decoder is then re-encoded and re-modulated in order to feedback to the next stages of the QR-SIC detector. The feedback symbol is used to remove its share of the interference from the other detected symbols in the QR-SIC detector. Probability of correct detection in the received symbols after the SIC detector is higher than the probability of correct detection in the corresponding symbols in the conventional QR-SIC detector

Fig. 1 shows the block diagram of the conventional SDM transmitter. The information bits are first encoded with the channel encoder. The coded bits are then modulated using an M-ary quadrature amplitude modulation (M-QAM) scheme. The output symbols from the modulator are shaped with a suitable shaping filter to limit the bandwidth of the transmitted signal to be smaller than the coherent bandwidth of the channel. The transmitter of the SDM system consists of M_t transmitting antennas. Each antenna transmits one modulated symbol

(S_{n,m_t}) every SDM symbol period. Equation (1) represents the n^{th} SDM symbol, which is transmitted from the SDM transmitter in the n^{th} symbol interval.

$$x\,(t - nT_s) = \sum_{m_t=1}^{M_t} S_{n,m_t} = \sum_{m_t=1}^{M_t} d_{n,m_t} p(t - nT_s)\colon n = 1, 2 \ldots N \quad (1)$$

N is the number of the SDM symbols. S_{n,m_t} is the transmitted symbol by the $m_t{}^{th}$ antenna in the n^{th} SDM symbol interval. M_t is the number of the transmitting antennas. T_s is the SDM symbol period. It is equal to the period of a modulated M-QAM symbol. d_{n,m_t} is the complex modulated M-QAM symbol, which is transmitted by the $m_t{}^{th}$ transmitting antenna in the n^{th} SDM symbol interval. Equation (2) shows the p(t) which is the impulse response of the raised cosine shaping filter. $p(t)$ represents the normalized shaping pulse of the transmitted symbols with a roll-off factor β.

$$p(t)) = \begin{cases} \frac{\pi}{4T_s}\operatorname{sinc}\left(\frac{1}{2\beta}\right) & t = \pm\frac{T_s}{2\beta} \\ \frac{1}{T_s}\operatorname{sinc}\left(\frac{t}{T_s}\right)\frac{\cos\left(\pi\frac{\beta t}{T_s}\right)}{1-\left(\frac{2\beta t}{T_s}\right)^2} & \text{elsewhere} \end{cases} \quad (2)$$

The spaces between the transmitting antennas are adjusted to be multiple of the transmitted signal wavelength. This reduces the cross coupling between the transmitting antennas and guarantees independent paths from the transmitter to the receiver [21]. Equation (3) shows the rate of the transmitted symbols R_s in the proposed SDM transmitter.

$$R_s = \frac{R_b}{r * (M) * M_t} \quad (3)$$

R_b is the information bit rate. M is the number of the constellation points in the used M-QAM modulation scheme. Equation (4) shows the bandwidth B_{SDM} of the transmitted SDM signal is equal to:

$$B_{\text{SDM}} = (1 + \beta)R_s \qquad 0 \leq \beta \leq 1 \quad (4)$$

β is the bandwidth expansion factor. It depends on the frequency response of the shaping filter. The channel model in this study is the flat-fading Rayleigh channel. The transmitted signal bandwidth B_{SDM} is adjusted to be always smaller than the coherent bandwidth of the Rayleigh fading channel.

The SDM receiver contains M_r receiving antennas. The number of the receiving antennas should be equal to the number of the transmitting antennas. The spaces between the receiving antennas are also multiple of the transmitted signal wavelength to guarantee independent fading paths from the transmitting antennas to the receiving antennas [5], [6], [23].

The conditions of the number of the receiving antennas and the spaces between these antennas ensure that the channel matrix is always a square matrix, and its rank is equal to the number of its rows and the number of its columns. Therefore, this channel matrix can be decomposed by the QR decomposition algorithm. Equation (5) shows the received signal by the m_r^{th} receiving antenna at the n^{th} SDM symbol interval.

$$r_{m_r}(t - nT_s) = \sum_{m_{t=1}}^{M_t} \propto_{m_{r,m_t}} . d_{n,m_t} \text{p (t} - \text{n}T_s) + w_{m_r}(t) \quad (5)$$

$\propto_{m_r,m_t}$ is a complex Gaussian random variable. It represents the fading gain from the $m_t{}^{th}$ transmitting antenna to the $m_r{}^{th}$ receiving antenna. $w_{m_r}(t)$ is a sample function of a white Gaussian noise process W(t). The mean of the noise sample function $w_{m_r}(t)$ is zero and its covariance function is $\sigma_W^2\,(t)$. The channel is assumed quasi-static. The fading gain is constant during the SDM symbol period T_s, and it randomly changes from one SDM symbol to another. A channel estimator is usually used in the receiver to estimate the fading gains. The structure of the channel estimator is out of the scope of this study. Perfect channel estimation is assumed and the channel status information (CSI) is always available to the receiver.

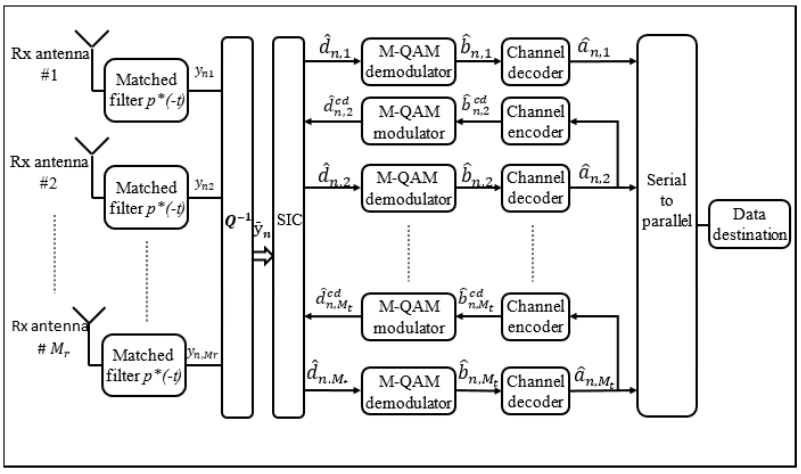

Fig. 2. A block diagram of the proposed SDM receiver with LDPC decoder

Fig. 2 shows the block diagram of the proposed SDM receiver. The first stage in the proposed SDM receiver is a group of M_r matched filters. The received signal from each receiving antennas passes through a filter matched to

the shaping pulse (t) of the transmitted symbols. The matched filters extract the maximum energy in the SDM symbol. Equation (6) shows the output of the m_r th matched filter due to the received signal in equation.

$$y_{m_r}(nT_s) = \int_{nT_s}^{(n+1)T_s} r_{m_r}(t - nT_s).p^*(t - nT_s).dt = \sum_{m_t}^{M_t} \propto_{m_r,m_t}.d_{n,m_t} + Z_{m_r} \quad (6)$$

Z_{m_r} is a complex Gaussian random variable with zero mean and σ_w^2 variance. The M_r outputs of the matched filters represent the elements of the input observation vector y_n to the QR-SIC detector. At the n^{th} SDM symbol, the observation vector y_n is indicated in equation (7) and is equal to:

$$y_n = H_n d_n + z_n \quad (7.a)$$

$$\begin{bmatrix} y_1(nT_s) \\ y_2(nT_s) \\ . \\ . \\ y_{M_r(nT_s)} \end{bmatrix} = \begin{bmatrix} \propto_{1,1} & \propto_{1,2} & \cdots & \propto_{1,M_t} \\ \propto_{2,1} & \propto_{2,2} & \cdots & \propto_{2,M_t} \\ \cdots & \cdots & \cdots & \cdots \\ \cdots & \cdots & \cdots & \cdots \\ \propto_{M_r,1} & \propto_{2,2} & \cdots & \propto_{M_r,M_t} \end{bmatrix} \begin{bmatrix} d_{n,1} \\ d_{n,2} \\ . \\ . \\ d_{n,M_t} \end{bmatrix} + \begin{bmatrix} Z_1 \\ Z_2 \\ . \\ . \\ Z_{M_r} \end{bmatrix} \quad (7.b)$$

The QR-SIC detector decomposes the channel matrix H_n into two matrices using the QR-decomposition algorithm. The first matrix is the Q_n matrix. It is an orthogonal matrix. The second matrix is the R_n matrix. It is an upper triangle matrix. In the first stage of the QR-SIC detector, the observation vector $y_n$is multiplied with the inverse of the Q_n matrix. Equation (8) shows the observation vector y_n after the mapping with the inverse $Q_n$matrix.

$$\bar{y}_n = Q_n^{-1}.\bar{y}_n = R_n d_n + V_n \quad (8.a)$$

$$\begin{bmatrix} \bar{y}_1(nT_s) \\ \bar{y}_2(nT_s) \\ . \\ . \\ . \\ \bar{y}_{M_r-1}(nT_s) \\ \bar{y}_{M_r}(nT_s) \end{bmatrix} = \begin{bmatrix} \rho_{1,1} & \rho_{1,2} & \cdots & \rho_{1,M_t-1} & \rho_{1,M_t} \\ 0 & \rho_{2,2} & \cdots & \rho_{2,M_t-1} & \rho_{2,M_t} \\ . & . & . & . & . \\ . & . & . & . & \\ 0 & 0 & \cdots & \rho_{M_r-1,M_t-1} & \rho_{M_r-1,M_t} \\ 0 & 0 & \cdots & 0 & \rho_{M_r,M_t} \end{bmatrix} \begin{bmatrix} d_{n,1} \\ d_{n,2} \\ . \\ . \\ . \\ d_{n,M_t-1} \\ d_{n,M_t} \end{bmatrix} + \begin{bmatrix} v_1 \\ v_1 \\ . \\ . \\ . \\ v_{M_{r-1}} \\ v_{M_r} \end{bmatrix} \quad (8.b)$$

The multiplication of the observation vector y_n with the inverse of the orthogonal matrix Q_n does not change the variance (the power) of the channel noise vector Z_n, because the Q_n matrix is a unitary matrix. The covariance matrix of the noise vector V_n is the same as the covariance matrix of noise vector Z_n as shown in equation (9).

$$cov(V_n) = E[V_n^H . V_n] = E[\ Z_n^H\ Q_n^{-H}.\ Q_n^{-1}\ Z_n] = [Z_n^H\ Z_n] = \sigma_W^2 I \quad (9)$$

() H is the Hermitian transpose of the matrix. According to equation (9), the noise samples in the observation vector $\bar{y}_n$ are independent. From equation (8.*b*), the last element in the mapped observation vector $\bar{y}_n$ is indicated in equation (10):

$$\bar{y}_{M_r}(nT_s) = \rho_{M_r,M_t}.d_{n,M_t} + v_{M_r} \quad (10)$$

By taking a closer look on this equation, it is found that there is no interference on symbol $d_{n,M_t}$from the other (M_t -1) M-QAM symbols in the n^{th} SDM symbol. The noise component v_{M_r} in equation (10) is a zero mean Gaussian random variable with the same variance of the channel noise component v_{Mr} in equation (7.b). Therefore $\bar{y}_{M_r}(nT_s)$ can be considered as the output from a matched filter in a conventional M-QAM receiver, which receives a signal transmitted through a Single-Input-Single-Output (SISO) flat fading channel. Maximum Likelihood (ML) demodulator is used to estimate the transmitted data symbol d_{n,M_t} in the n^{th} SDM symbol interval as shown in equation (11).

$$\hat{d}_{n,M_t} = arg(\min_{d_i} |\ \bar{y}_{Mr}(nT_s) - \rho_{M_r,M_t}.d_i|^2\ ) \quad (11)$$

In the conventional QR-SIC detector, the estimated symbol $\hat{d}_{n,M_t}$ from this stage is feedback to the up stages in the QR-SIC detector to remove its interference share from the rest ($M_t - 1$) symbols in the symbols vector d_n. For example, equation(12) shows the symbol number (M_t-1) in the observation vector $\bar{y}_n$ which is equal to:

$$\bar{y}_{M_r-1}(nT_s) = \rho_{M_r-1,M_t-1}.d_{n,M_t-1} + \rho_{M_r-1,M_t}.d_{n,M_t} + v_{M_{r-1}} \quad (12)$$

The modulated symbol d_{n,M_t-1} in the observation vector $\bar{y}_n$ merely suffers the interference from the modulated symbol d_{n+M_t} and the noise component $v_{M_{r-1}}$. The estimated symbol $\hat{d}_{n,M_t}$from the first stage in the QR-SIC detector in equation (11) is feedback and subtracted from $\bar{y}_{M_r-1}(nT_s)$ after multiplying with the channel fading gain ρ_{M_r-1,M_t}. The ML demodulator is then used to estimate the modulated symbol d_{n,M_t-1} from the subtraction result as shown in equation (13).

$$\hat{d}_{n,M_t-1} = arg(\min_{d_i} |\ \bar{y}_{Mr}(nT_s) - \rho_{M_r-1,M_t}.\hat{d}_{n,M_t} - \rho_{M_r-1,M_t-1}.d_i|^2 \quad (13)$$

The same process is repeated for the next stages in the QR-SIC detector until all the symbols in the SDM vector

d_n are estimated. Equation (14) shows the ML demodulation for the arbitrary symbol d_{n,M_t} where m_t =m_r.

$$\hat{d}_{n,M_t} = \arg\left(\min_{d_i}|(\bar{y}_{Mr}(n.T_s)\sum_{m=M_t}^{m_t-1}\rho_{m_r,m}.\hat{d}_{n,m}) - \rho_{m_r,m_t}.d_i|^2\right) \quad (14)$$

The estimated symbol $\hat{d}_{n,M_t}$ is then mapped to a binary symbol $\hat{b}_{n,M_t}$ using the baseband M-QAM detector. In the convention SDM receiver, the estimated binary symbols enter the channel decoder to correct the errors in the detected symbols due to the residual interference and the channel noise. The channel decoder can correct up to *t* error in each code word. *t* is related to the minimum distance of the channel code according to equation (15).

$$t = \lfloor\frac{1}{2}(d_{min} - 1)\rfloor \quad (15)$$

$\lfloor x\rfloor$ is the floor of the real number *x*.

In the proposed SDM receiver, the feedback in the $m_t{}^{th}$ stage of the QR-SIC detector is not done using the estimated symbols ($\hat{d}_{n,M_t}$, $\hat{d}_{n,M_t-1}\ldots\hat{d}_{n,m_t-1}$) from the previous stages. However, the feedback is done using the estimated symbols after the channel decoder as shown in Fig. 2. The probability of error in the estimated symbols after the channel decoder is less than the probability of error in the estimated symbols after the QR-SIC detector. Therefore, the feedback in the proposed receiver is done using symbols that are more robust. The binary symbols after the channel decoder are re-encoded and re-modulated before they are feedback to the QR-SIC detector. The new symbols used to estimate the d_{n+m_t} in the $m_t{}^{th}$ stage of the QR-SIC detector are ($\hat{d}^{cd}_{n,M_t}$, $\hat{d}^{cd}_{n,M_t-1}$, …, $\hat{d}^{cd}_{n,m_t-1}$)as shown in Fig. 2. Equation (16) shows the ML demodulation for the symbol d_{n+m_t} using the more robust estimated symbols from the channel decoder.

$$\hat{d}_{n,m_t} = \arg\left(\min_{d_i}|(\bar{y}_{Mr}(n.T_s)\sum_{m=M_T}^{m_t-1}\rho_{m_r,m}.\hat{d}^{cd}_{n,m}) - \rho_{m_r,m_t}.d_i|^2\right) \quad (16)$$

$\hat{d}^{cd}_{n,m}$ is the m^{th} feedback symbol from the m^{th} QR- SIC stage after the channel re-encoding and the M-QAM re-modulating to the output symbol from the m^{th} channel decoder. The improvement in the probability of error in the proposed receiver architecture comes on the expense of the system latency and complexity. However, the using of high-speed digital signal processors or parallel processing algorithms may overcome the increase in the system latency. Moreover, the big development in the integrated circuit technologies and the increase in the densities of FPGA and ASIC chips can absorb the added modulators and channel encoders in the feedback paths.

The residual power of the interference and noise in the output of the $m_r{}^{th}$ stage in the QR-SIC detector is equal to the difference between the power of the output of the QR-SIC detector in this stage and the power of the modulator output in the $m_t{}^{th}$ stage in the transmitter. By subtracting the noise power from this difference, the resultant represents the residual interference in the detected symbols after the QR-SIC detector. Equation (17) shows the residual interference power p_{RI} in the detected symbol from $the\ m_r{}^{th}$ stage in the proposed QR-SIC detector.

$$(p_{RI})_{m_r} = |(\bar{y}_{mr}(nT_s) - \sum_{m=M_T}^{m_t-1}\rho_{m_r,m}.\hat{d}^{cd}_{n,m}) - \rho_{m_r,m_t}.d_{n,m_t}| - \sigma_W^2 \quad (17)$$

III. The Proposed Channel Code for the SDM System

The channel coding reduces the bit-error-rate (BER) in the received information symbols. The systems with high noise and interference powers use channel codes with small code rates to overcome the noise and the interference effects. When the noise and the interference powers are small, channel codes with higher code rates are used. Each channel code has a specific code gain at a certain BER. It represents the difference between the received signal to noise and interference ratios SNIR of the coded system and the un-coded system at a certain BER. In conventional systems, the interference cancellation process and the channel decoding process are independent. The interference cancellation detector removes or minimizes the interference at its output according to its operating criterion. The channel decoder then corrects some of the errors in the output symbols from the interference cancelation detector according to its correction capability. There is no feedback information between the channel decoder and the interference cancellation detector.

The channel codes with high code gains such as the low-density parity check (LDPC) code and the turbo code are recommended in the proposed receiver, because the signal to interference ratio is low in the SDM system. The LDPC is more preferred because its encoder is simpler than the encoder of the turbo codes is. Channel codes with simpler encoder reduce the latency of the feedback path and the detection time of the next symbols in the proposed QR-SIC detector. The encoder of the LDPC code multiplies the message vector with the generator matrix **G** as shown in equation (18).

$$\mathbf{c} = \mathbf{m}.\mathbf{G} \quad (18)$$

m is a row vector of *k* message bits. **G** is the generator matrix of the LDPC code. It is consisting of *k* rows and *n* columns. **c** is a row vector of *n* coded bits. The code rate of the used LDPC code is *k*/*n*. The LDPC encoder is implemented with two methods. The first method uses logic gates to implement the multiplication between the message vector and the columns of the generator matrix **G**. *n* groups of *k* AND gates are used to do the modulo-2 multiplication between the message word and the columns in the generator matrix **G**. *n* XOR gates are used to do the modulo-2 summation between the output *k* bits from the (AND) gates in each group. The second way of the

implementation of the LDPC encoder uses a look-up table (LUT) to save the code word according to equation (18). The message word is used as an address to the LUT, and the code word is the data gotten from the LUT. This method is preferred when the number and the size of the message words and the code words are small. However, the first method is preferred when the number and the size of the message words and the code words are big. The LDPC code is defined by the parity-check matrix H. Since the LDPC code is a linear block code, the rows space of its generator matrix G is the null space of its parity-check matrix H [24]. Equation (19) represents the condition, which should be satisfied by the generator matrix G and the parity-check matrix H of any linear block code.

$$\mathbf{G}.H^T=0 \tag{19}$$

In this proposal, a new algorithm for generating the LDPC parity check matrix is proposed. The proposed algorithm creates the parity-check matrix randomly. The created **H** matrix is a regular matrix, which should satisfy the following condition in equation (20):

$$\frac{W_c}{W_r} = 1 - r \tag{20}$$

w_c are the columns weights of the **H** matrix. w_r is the rows weights of the **H** matrix. r is the code rate. The proposed **H** matrix is constructed according to the following steps:

1-The rows of the **H** matrix are divided into l groups. Each group consists of m rows.

2-The number of rows in each group is specified by equation (21):

$$\text{m}= \frac{n}{w_r} \tag{21}$$

3-Each row in each group contains w_r ones assigned randomly to w_r locations in the n columns.

4-No two or more rows in the same group have one in the same column location.

Therefore, the weight of each column in each group is one.

5-The weight of the columns w_c in the **H** matrix can be calculated by equation (22):

$$W_{c=} \quad _L \frac{n-k}{m} \tag{22}$$

If equation (21) is substituted in equation (22), the condition is equation (20) will be obtained. Therefore, the proposed algorithm will produce a regular **H** matrix for the LDPC code. The code vectors in the proposed LDPC code must satisfy the check equation of the linear block codes as shown in equation (23).

$$\mathbf{c}.\ H^T = \mathbf{0} \tag{23}$$

Since the minimum distance of the linear code is equal to the minimum Hamming weight of non-zero code vector, the minimum distance is equal to the minimum number of columns in the **H** matrix whose sum is equal to the zero vector. Therefore, it is preferred to assign an even row weight for the **H** matrix according to proposed algorithm.

IV. The Simulation Results and the Discussion

In this section, the proposed SDM receiver is simulated at different channels and system conditions. The information rate R_b in the simulated systems is 10 M bits/s.

TABLE I: THE BANDWIDTH OF THE TRANSMITTED SDM SIGNALS IN THE SIMULATED SYSTEMS

8-antennas SDM system	4-antennas SDM system		
Code rate = 1/2	Code rate = 1/4	Code rate =1/2	Code rate = 3/4
BW=688 KHz	BW=2.75 MHz	BW=1.38 MHz	BW=917 KHz

Two SDM systems are simulated. The first uses four transmitting antennas and the other uses eight transmitting antennas. Convolution code, turbo code and LDPC code are used in the simulations of the two proposed SDM systems. The code rates of the used convolution codes are 1/4, 1/2 and 3/4. For LDPC code, the proposed random algorithm is used to generate the parity check matrix **H** of the code. The code rate of the used LDPC code is 1/2. The decoder of the LDPC is implemented using the Sum-Product algorithm. Turbo code with code rate 1/2 is also used in the simulations. The decoder of the turbo code is implemented using the BCJR algorithm. The simulated systems use 16-QAM modulation and raised-cosine shaping filter with 0.1 roll-off factor. Table I shows the bandwidths of the transmitted SDM signals in the simulated systems using equations (3) and (4). For 4-antenna SDM system, by increasing the code rate from ¼,1/2,3/4 the transmitted signal bandwidth of SDM system decreases. Also the 8-Antenna SDM system is studied for ½ code rate.

From [23], [25], the simulated flat-fading Rayleigh channels have average coherent bandwidths of 700KHz for urban outdoor channel and 2.8 MHz for indoor channel. The 4-antennas SDM system is simulated with the indoor channel model, however the 8-antennas SDM system is simulated with the outdoor channel model. It is assumed that all the transmitted symbols from the transmitting antennas have the same power levels. The signal to interference ratio (SIR) at the inputs of the 4-antennas SDM receiver is -4.771 dB and at the inputs of the 8-antennas SDM receiver is -8.45 dB

Fig. 3 shows the BER performance of the 4-antennas SDM receiver. QR-SIC detector is used to remove the interference between the received symbols. The 4-antennas SDM receiver is simulated without channel coding and with convolution codes of rates 1/4, 1/2, and 3/4. The BER performance of the simulated SDM receiver is also compared with the BER performance of the SISO receiver in flat fading Rayleigh channel.

From Fig. 3, it is observed that the BER performance of the uncoded 4-antennas SDM receiver with QR-SIC detector is 3 dB worse than the BER performance of the SISO receiver. Since the SIR at the receiver inputs is -4.771 dB, the QR-SIC detector approximately removes 1.771 dB of the power of the interfering signals. The power of the remaining interfering signals at the output of the QR-SIC detector is 3 dB. This remaining interference power is the source of the 3dB difference between the BER performance of the uncoded 4-antennas SDM receiver and the SISO receiver.

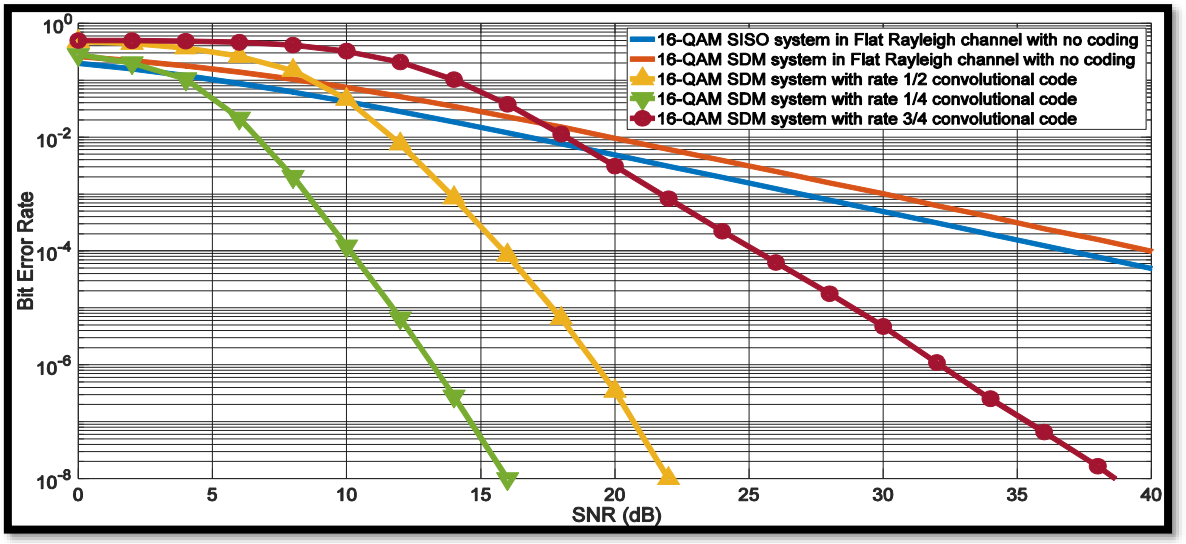

Fig. 3. Conventional 16-QAM 4-antennas SDM system without coding and with rate 1/4, 1/2, and 3/4 convolution code in Rayleigh flat fading channel

When channel codes are used, they enhance the performance of the SDM receiver significantly. At BER of 10^{-4}, the convolution codes of code rates 3/4, 1/2, and 1/4 achieve coding gains of 15 dB, 24 dB, and 30 dB with respect to the uncoded 4-antennas SDM receiver, respectively. These code gains increases when the BER decreases.

Fig. 4. shows the BER performance of the proposed SDM receiver when the feedback in the QR-SIC detector is done by the symbols after the channel decoder as shown in Fig. 2. The BER performance of the proposed SDM receiver is compared with the BER performance of the conventional coded SDM receiver when the feedback in the QR-SIC detector is done by the symbols before the 16-QAM demodulator.

It is observed from Fig. 4 that the performance of the proposed SDM receiver at BER of 10^{-4} is 2dB, 1.5 dB, and 0.9 dB better than the BER performance of the conventional coded SDM receiver at code rates 1/4, 1/2, and 3/4 convolution codes, respectively. The enhancement in the BER performance of the proposed SDM receiver increases as the code gain of the used code increases. This is logical because the probability of error in the feedback symbols to the QR-SIC detector decreases when the code gains of the used channel code increases. Therefore, the interference cancellation in the QR-SIC detector is done using symbols that are more robust.

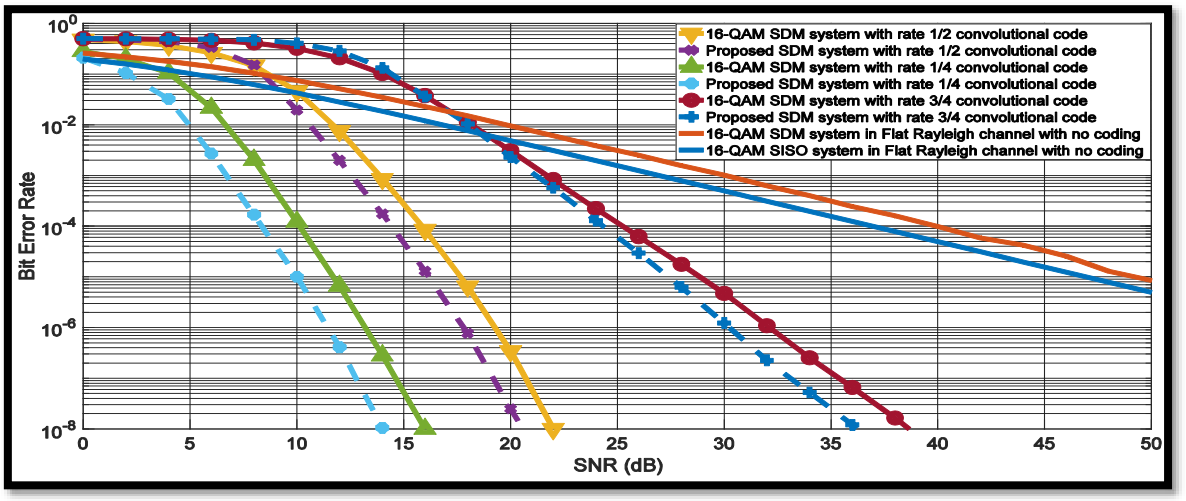

Fig. 4. Conventional 16-QAM 4-antennas SDM system with rate 1/4, 1/2, and 3/4 convolution code and the proposed 16-QAM 4-antennas SDM system with the same code rates in Rayleigh flat fading channel

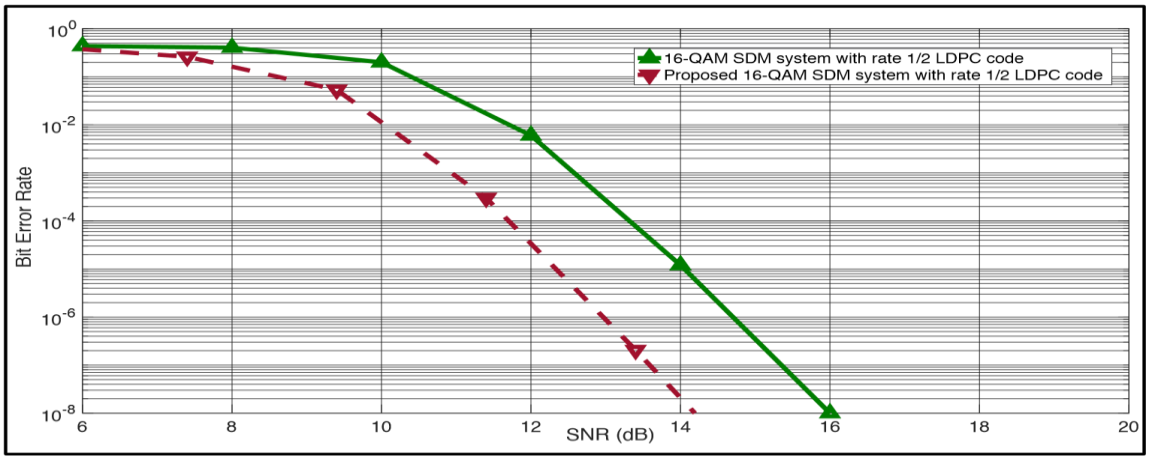

Fig. 5. Conventional 16-QAM 4-antennas SDM system with rate 1/2 (16 iteration) LDPC code and the proposed 16-QAM 4-antennas SDM system with the same code rate and decoding iteration number in Rayleigh flat fading channel

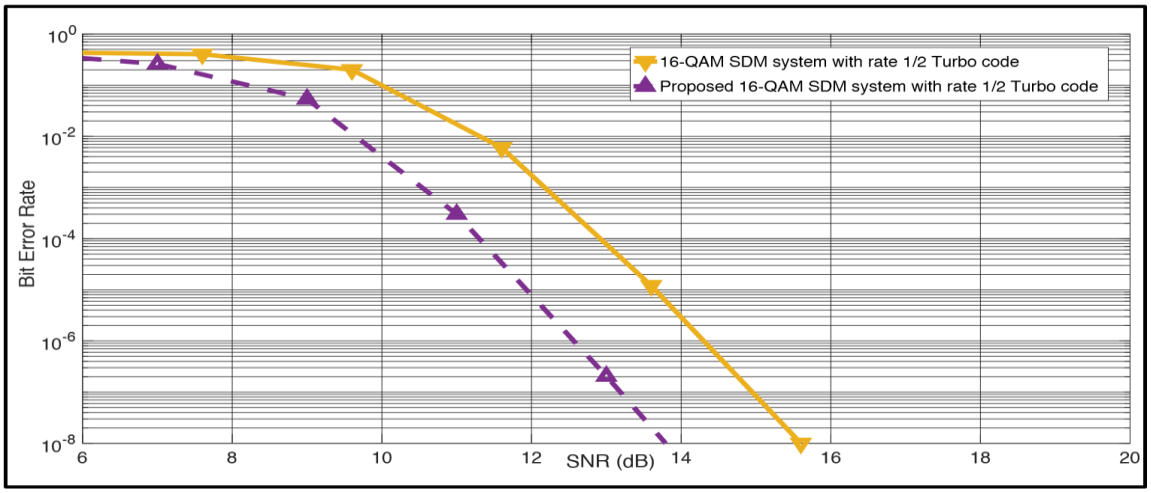

Fig. 6. Conventional 16-QAM 4-antennas SDM system with rate 1/2 (8 iteration) Turbo code and the proposed 16-QAM 4-antennas SDM system with the same code rate and decoding iteration number in Rayleigh flat fading channel

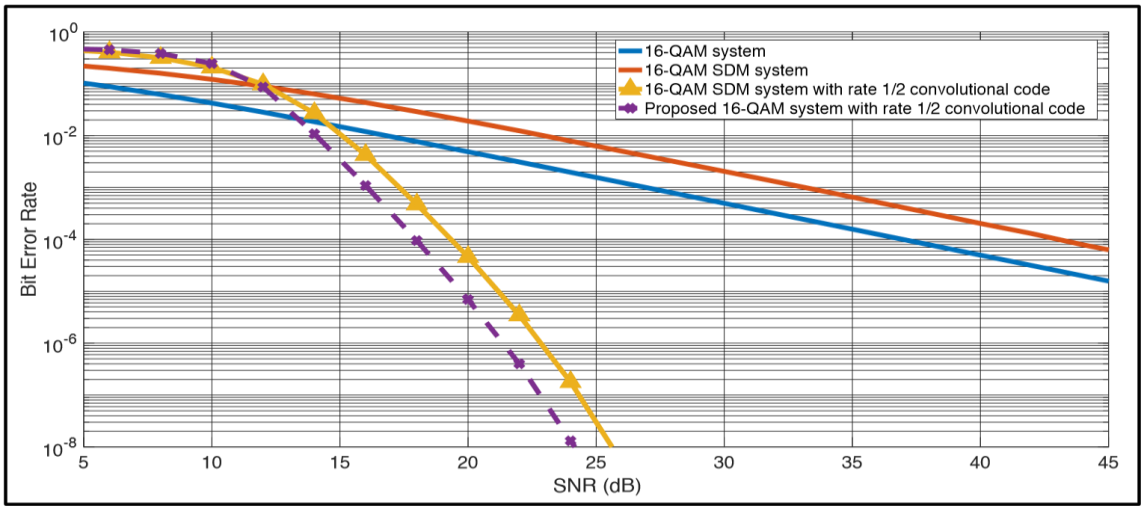

Fig. 7. Conventional 16-QAM 8-antennas SDM system without coding and with rate ½, convolution code and the proposed 16-QAM 8-antennas SDM system with the same code rate in Rayleigh flat fading channel

Fig. (5) shows the BER performance of the conventional coded 4-antennas SDM receiver and the proposed 4-antennas SDM receiver when LDPC code is used. The BER performance of the proposed SDM receiver is also better than the BER performance of the conventional coded SDM receiver by approximately 1.5 dB at BER of 10^{-4}. The same result is observed in figure (6) when Turbo code is used instead of the LDPC code. At BER of 10^{-4}, the BER performance of the proposed 4-antennas SDM receiver with turbo code is better than the

BER performance of the conventional coded SDM receiver with turbo code by approximately 1.7 dB

Fig. 7, Fig. 8, and Fig. 9 show the simulation results of the proposed and the conventional 8antennas SDM system in urban outdoor flat fading Rayleigh channel. The SIR ratio at the inputs of the 8-antennas is -8.45 dB

Fig. 7 shows the BER performance of the uncoded 8-antennas SDM receiver with QR-SIC detector compared with the BER performance of the SISO system in the same fading channel. It is observed form figure (7) that the BER performance of the uncoded 8-antennas SDM receiver is -6 dB worse than BER performance of the SISO receiver. The QR-SIC detector removes 2.45 dB of the power of the interfering signals at its input. The remaining interference power at the output of the QR-SIC detector is 6 dB

Fig. 7 also shows the BER performance of the coded SDM receiver and the proposed SDM receiver when convolution code with rate 1/2 is used. The BER performance of the conventional coded SDM receiver is enhanced by approximately 23 dB than the BER performance of the uncoded SDM receiver at BER of 10^{-4}. Moreover, the proposed SDM receiver achieves an enhancement of approximately 1.5 dB than the BER performance of the conventional coded SDM receiver. This enhancement factor is the same as the enhancement factor in the BER performance of the proposed 4-antennas SDM receiver in the previous indoor simulation.

Fig. 8 and Fig. 9 show the comparisons between the BER performance of the coded 8antennas SDM receiver and the proposed 8-antennas SDM receiver when LDPC code and turbo code are used, respectively. At BER of 10^{-4}, the proposed SDM receiver with LDPC code achieves an enhancement in the BER performance of the coded 8-antennas SDM receiver with LDPC code by 1.4 dB However, when turbo code is used, the proposed SDM receiver achieves an enhancement in the BER performance by 1.6 dB

Form the simulations of the proposed 4-antennas SDM receiver and 8-antennas SDM receiver; it is observed that the enhancement in the BER performance does not depend on the number of the transmitting and receiving antennas. The BER performance enhancement in the proposed receiver architecture depends only on the coding gain of the used channel codes.

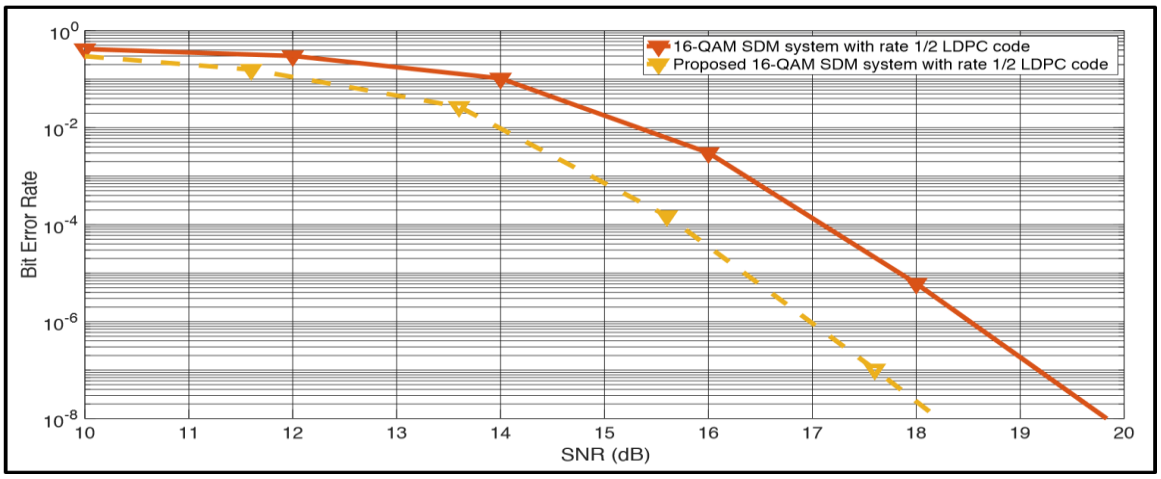

Fig. 8. Conventional 16-QAM 8-antennas SDM system with rate ½ (16 iteration) LDPC code and the proposed 16-QAM 8-antennas SDM system with the same code rate and decoding iteration number in Rayleigh flat fading channel

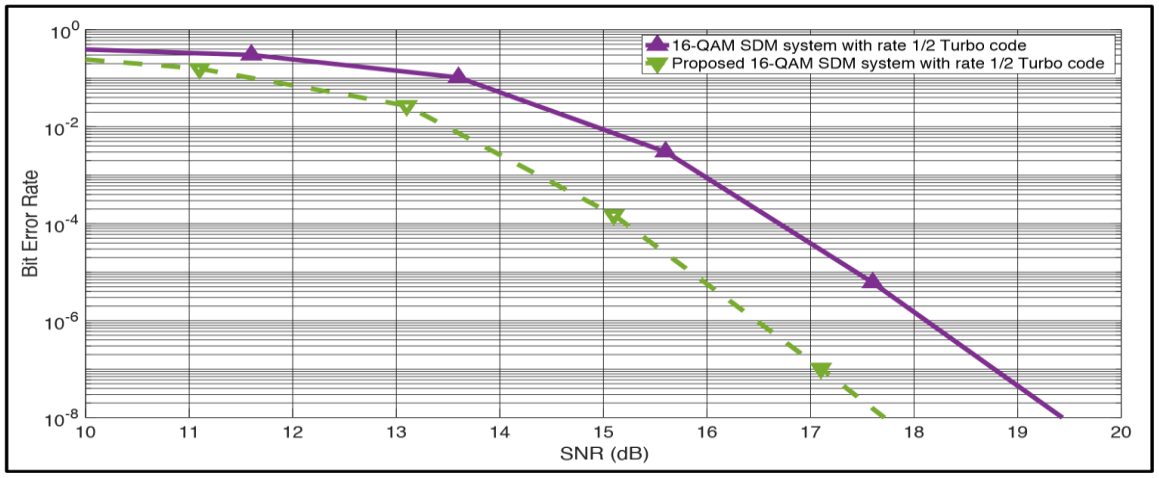

Fig. 9. Conventional 16-QAM 8-antennas SDM system with rate 1/2 (8 iteration) Turbo code and the proposed 16-QAM 8-antennas SDM system with the same code rate and decoding iteration number in Rayleigh flat fading channel

V. Conclusion

The SDM systems increases the data transmission rate, but it suffers from high interference between the received symbols. The QR-SIC detector is linear detector, which is used to remover the interference in the SDM receiver. In the same flat fading channel, the BER performance of the 4-antennas SDM receiver and the 8-antennas SDM receiver are worse than the BER performance of the SISO receiver by 3 dB and 6 dB, respectively. The channel coding greatly enhances the performance of the SDM receiver with the QR-SIC detector. The convolution code, the LDPC code, and the turbo code with rate 1/2 achieve coding gains of 24 dB, 26.5 dB, and 27 dB at BER of 10^{-4}, respectively. In the conventional SDM receiver, the feedback symbols to the QR-SIC detector are done using the detected symbols from the previous stages of the QR-SIC detector. The BER performance of the SDM receiver can be more enhanced when the output symbols from the channel decoder are feedback to the QRSIC detector after re-encoding and re-modulation. The probability of error in the received symbols after the channel decoder is smaller than the probability of error in the received symbols after the QR-SIC detector. Therefore, the feedback symbols in the proposed QR-SIC detector are more robust than the feedback symbols after the QR-SIC detector, which are used in the conventional SDM receiver. For the indoor flat fading channel, the proposed 4antennas SDM receiver can save 36%, 30%, and 19% of the transmitted signal power in the conventional 4-antennas SDM system when convolution codes with rates 1/4, 1/2, and 3/4 are used. The power saving in the BER performance of the proposed 4-antennas SDM receiver is with respect to the conventional 4-antennas SDM receiver with the same channel code and the same code rate. Moreover, the proposed 4-antennas SDM receiver can save 33% and 30% of the transmitted signal power if the turbo code and LDPC code with rate 1/2 are used, respectively. For the outdoor flat fading channel, the proposed 8-antennas SDM receiver can save 31%, 30%, and 28% of the transmitted signal power in the conventional 8-antennas SDM system if turbo code, convolution code, and LDPC code with code rate 1/2 are used, respectively. The power saving in the BER performance of the proposed 8-antennas SDM receiver is also with respect to the conventional 8-antennas SDM receiver with the same channel code and the same code rate. By comparing the results of the proposed 4-antennas SDM receiver and 8-antennas SDM receiver, the BER performance of the proposed SDM receiver does not depend on the number of the used antennas, however it merely depends on the code gain of the used channel code. Also if the system is applied to slow and fast fading channel to compare its performance. For fast fading channels due to the relative mobility between the transmitter and receiver, the BER increases more than the BER in slow fading channels. The proposed system will improve the BER for fast fading channels by the same amount of coding gain () of the used channel code. The coding gain is a function in the used code rate and type of the channel code. The coding gain is not affected by the channel characteristics.

Conflict of Interest

The authors declare no conflict of interest.

Author Contributions

Through regular discussion, all authors contributed to the paper. Ashraf yehya developed the idea with Heba Talla Adel. They performed the data analysis and worked on the practical points. Abdelhalim reviewed the content of the paper. All authors had approved the final version.

References

[1] A. Y. Hassan, "Enhancing signal detection in frequency selective channels by exploiting time diversity in inter-symbol interference signal," *Wireless personal Communications* (Springer), vol. 106, no. 3, pp. 1373–1395, June 2019.

[2] R. Zakaria and D. Le Ruyet, "Intrinsic interference reduction in a filter bank-based multicarrier using QAM modulation," *Physical Communication*, vol. 11, pp. 15-24, June 2014.

[3] A. Y. Hassan, "Minimizing the effects of inter-carrier interference signal in OFDM system using FTMLE based algorithm," *Wireless personal communications (Springer)*, vol. 97, no. 2, pp. 1997–2015, November 2017.

[4] L. Ma, W. Jiang, and H. Xiang, "Reception and detection of a wide-band OFDM signal in a Doppler spreading channel," *IET Communications*, vol. 12, no. 9, pp. 1134-1140, 2018.

[5] L. A. Dalton and C. N. Georghiades, "A full-rate, full-diversity four-antenna quasi-orthogonal space-time block code," *IEEE Transactions on Wireless Communications*, vol. 4, no. 2, pp. 363–366, March 2005.

[6] B. Vucetic and J. Yuan, *Space Time Coding*, Wiley, 1st edition, 2003.

[7] T. H. Liu, "Analysis of the Alamouti STBC MIMO system with spatial division multiplexing over the Rayleigh fading channel," *IEEE Transactions on Wireless Communications*, vol. 14, no. 20, pp. 5156-5170, May 2015.

[8] A. Maaref and S. Aissa, "Capacity of space-time block codes in MIMO Rayleigh fading channel with adaptive transmission and estimation errors," *IEEE Transactions on Wireless Communications*, vol. 4, no. 5, 2005, pp. 2568-2578.

[9] D. Sim, K. Kim, C. Kim, and C. Lee, "A signal-level maximum likelihood detection based on partial candidates for MIMO FBMC-QAM system with two prototype filters," *IEEE Transactions on Vehicular Technology*, vol. 68, no. 3, pp. 2598-2608, 2019.

[10] Y. Hama and H. Ochiai, "A low-complexity matched filter detector with parallel interference cancellation for massive MIMO systems," *Proc. IEEE WiMob*, Oct. 2016.

[11] J. GuEmail and R. C. D. Lamare, "Joint interference cancellation and relay selection algorithms based on greedy techniques for cooperative DS-CDMA systems," *EURASIP Journal on Wireless Communications and Networking*, 2016.
[12] L. Fang, L. Xu, and D. Huang, "Low complexity iterative MMSE-PIC detection for medium-size massive MIMO," *IEEE Wireless Communication Letters*, vol. 5, no. 1, pp. 108-111, 2016.
[13] A. Salhb, L. Audaha, N. S. M. Shahc, and S. A. Hamzahd, "A study on the achievable data rate in massive MIMO System," September 2017.
[14] B. Ling, *et al*., "Multiple decision aided successive interference cancellation receiver for NOMA systems," *IEEE Wireless Communication Letters*, vol. 6, no. 4, pp. 498-501, Aug. 2017.
[15] M. F. Uddin and S. Mahmud, "Carrier sensing based medium access control protocol for WLANs exploiting successive interference cancellation," *IEEE Transactions on Wireless Communications*, vol. 16, no. 6, pp. 41204135, June 2017.
[16] M. A. Albreem, M. Juntti, and S. Shahabuddin, "Massive MIMO Detection Techniques: A Survey," August 2018.
[17] M. Mandloi, M. A. Hussain, and V. Bhatia, "Improved multiple feedback successive interference cancellation algorithms for near-optimal MIMO detection," *IET Communications*, vol. 11, no. 1, pp. 150-159, Jan. 2017.
[18] R. F. H. Fischer, C. Stierstorfer, and R. R. Müller, "subspace projection and noncoherent equalization in multiuser massive MIMO systems," in *Proc. International ITG Conference on Systems Communications and Coding*, Feb. 2015, pp. 1-6.
[19] P. Li and R. C. D. Lamare, "Adaptive decision-feedback detection with constellation constraints for mimo systems," *IEEE Transactions on Vehicular Technology*, vol. 61, no. 2, pp. 853-859, February 2012.
[20] P. Li, R. C. D. Lamare, and J. Liu, "Adaptive decision feedback detection with parallel interference cancellation and constellation constraints for multiuser multi-input-multi-output systems," *IET Communications*, vol. 7, no. 6, pp. 538-547, December 2013.
[21] Naeem, Muddasar, *et al*., "Application of reinforcement learning and deep learning in Multiple-Input and Multiple-Output (MIMO) Systems," *Sensors*, vol. 22, no. 1, p. 309, Dec. 2021.
[22] Q. MengJia, X. Zhao, W. Xu, and L. Li, "A construction of the high-rate regular quasi-cyclic LDPC codes," *EURASIP Journal on Wireless Communications and Networking*, December 2019.
[23] T. S. Rappaport, *Wireless Communications: Principles and Practice*, 2nd Edition, Prentice Hall, 2 editions January 10, 2002.
[24] S. Lin and D. J. Costello, *Error Control Coding*, Pearson; 2nd edition, June 7, 2004.
[25] J. Proakis and M. Salehi, *Digital Communications*, McGraw-Hill, 2008.

Heba Talla Adel Ebrahem Electronic engineer in EETC (Egyptian electricity transmission company), Communication engineering (June 2008), grade very good with honor 83% graduation, graduation project in ground penetrating radar with excellent degree, Master student at Benha faculty of engineering.

Ashraf Y. Hassan received the B.Sc. degree (with honor) and the M.S. degree in electrical engineering from, Benha University, Benha, Egypt, in 2000 and 2004, respectively, and the PhD degree in Electronics and Electrical Communications Engineering from Cairo University, Cairo, in 2010. From 2000 to 2010, he served as a research and teaching assistant at the electrical technology department in Benha Faculty of Engineering. At 2010, he employed as an assistant professor in electronics and communication engineering in the electrical engineering department. He works nine years as a researcher in the research and development center in Egyptian Telephone Company from 2000 to 2009. From 2012 until 2015, he works as a visiting assistant professor at Northern Border University – Faculty of Engineering, Saudi Arabia. In 2017, he has promoted to associated professor degree. Now he was the head of the electrical engineering department from 2017 to 2019 in Benha faculty of engineering – Benha University, Egypt. Now he is the head of a research group working in physical layer researches for new communication standards such as 5G, DVB-S2, and ISDB-S3 standards. His current research interests include detection and estimation theory, digital communication systems, modelling of time-varying channels, interference cancellation techniques, signal processing, coding for high-data-rate wireless and digital communications and modem design for broadband systems.

Abdelhalim Zekry is Professor of Electronics and Communication Engineering at Ain Shams University, Cairo, Egypt, (and previously at King Saud University), where he is also the head of the Communication and Electronics laboratory. He has over 50 years of academic and industrial experience including conducting high-quality research, teaching advanced courses, and consulting dozens of companies and government agencies throughout his career. He obtained his Ph.D. in Electrical Engineering from the Technical University of Berlin, Germany, in 1981, and he has supervised more than 110 Master theses and 40 Ph.D. theses at several universities. In

addition, he founded and established the Microelectronic Research and Development Unit at the Fac. of Eng., ASU. He also established the electronics for communications laboratory for designing, implementing, and testing the building blocks of the advanced electronic communication systems according to the ITU standards. He has authored more than 350 papers along with writing more than 7 books published by several international organizations. He has received dozens of grants and awards as recognition for his contributions to the research community. Due to this contribution, which has proven to be extremely impactful and useful for researchers worldwide, Prof. Abdelhalim's profile has been ranked number at the top of among all researchers on the Research gate platform in the world.

His research topics cover communication technologies, semiconductor materials, semiconductor devices, microelectromechanical devices, electronic circuits, solid-state circuits, solar cells, solar systems, photoelectrochemical devices, and applications in hydrogen production as well as communication and electronics.